

CROPS 2017

Young scientists Chinese-Russian Optics & Photonics Symposium

CONFERENCE ABSTRACTS

St.Petersburg

Table of contents

Measurement of a condition of polarization of optical beams, method Stokes polarimetry, in real time	1
The study of compacted singular beam transmitted in few-mode fiber	4
Simultaneous assessment of blood flow rhythmic oscillation by using of laser Doppler flowmetry and videocapillaroscopy methods	7
Design and implementation of wavefront aberration correction by liquid crystal spatial light modulator	8
Influence of silicon resonant particles on the surface plasmon-polaritons excitation efficiency	9
An optimized design of miniaturized terahertz time-domain spectrometer	11
Modeling of self-consistent modes in optical fibers with $V=3.8$	12
Free Space OTDM System based on Pulse Width Compression of Supercontinuum	16
Generation of microwave vortex field	17
Optical vortex profilometry with nanoscale resolution	20
Holographic formation and properties of hybrid surface-relief/volume periodic structures	23
Assessment of the influence of different concentrations of zinc on the brain biochemical processes in rat model	24
Demonstration of free space optical transmission in weak turbulence based on partially coherent sources in a novel method	25
Study on Frequency Domain Characteristics Measurement of Pulse Signal in Atmosphere Laser Communication	26
A novel continuous-terahertz-wave molecular imaging method for biomedical applications	27
Study on bionic compound eyes imaging system in field stitching method	29
Laser Doppler flowmetry and spectroscopy methods in assessment of microvascular and metabolic complications in diabetes	30
Octagonal-core and nodeless anti-resonant hollow-core fibers transmission spectra comparison	31
Application and possibilities of fluorescence spectroscopy method for intraoperative analysis of abdominal cavity organs tissues during minimally invasive interventions	33
Blood glucose concentration sensing using THz spectroscopy	35

Measurement of a condition of polarization of optical beams, method Stokes polarimetry, in real time

A O Kovalyova¹, A F Rubass¹

¹V.I. Vernadsky Crimean Federal University, Vernadsky Prospekt, 4, Simferopol, 295007, Russian Federation.

E-mail: kurioza.9@gmail.com

Abstract. The technical solution of the method proposed by us relates to the field of optics for the development and creation of the optical devices allowing to measure a condition of polarization of inhomogeneously polarized monochromatic light fields in real time. It can be used and applied in polarimetry to study the structure and properties of substances in the optical industry to improvement the quality and reliability of polarized optical instruments of polarizing optical devices

1. Introduction

In recent years, the technology of "augmented reality" is developing [1, 2], allowing to expand the range of data perceived by a person. Devices and applications modeled on this technology, greatly simplify the process of collecting and processing information. The model proposed by us can be used in the field of optics for the development and creation of optical instruments that allow measuring the state of polarization, using the Stokes polarimetry method [3], inhomogeneously polarized monochromatic light fields, in real time. The drawback of the previously proposed technical solution [4] is the laboriousness of the process of obtaining a polarization distribution, in which the measurement of intensity profiles is carried out in stages, rather than in real time. In practice, this method is not as convenient as the utility model that we proposed.

2. The energy representation of the light signal described by the Stokes parameters

It is known that to define a condition of polarization, the light beam of a completely polarized and partially polarized, it is convenient by means of Stokes parameters. The Stokes parameters can be represented in the form:

S_0 - the full capacity of a light signal average on time, power polarized and unpolarized a component.

S_1 - the difference between the power of linear horizontal and linear vertical polarization components of the light signal.

S_2 - the difference between the power of the linear 45° and linear -45° polarization components of the light signal.

S_3 - the difference between the power of the circular right-hand and circular left-handed polarization components of the light signal.

The Stokes parameters describe the light signal in the energy representation, which gives additional convenience in the experimental study - the current of the photodetector is proportional to the power of the received optical radiation. The powers of the polarized and unpolarized light components are, respectively, $\sqrt{S_1^2 + S_2^2 + S_3^2}$ and $S_0 = \sqrt{S_1^2 + S_2^2 + S_3^2}$. The degree of polarization SOP (accepts values from 0 to 1) is the ratio of the power of the polarized part of the radiation to the total radiation power $SOP = \frac{\sqrt{S_1^2 + S_2^2 + S_3^2}}{S_0}$. Along with S_1 , S_2 , and S_3 use also the normalized Stokes parameters

$s_1 = S_1/S_0$, $s_2 = S_2/S_0$ and $s_3 = S_3/S_0$. For polarized light $s_1^2 + s_2^2 + s_3^2 = 1$. Thus, if we introduce a Cartesian coordinate system with the axes s_1 , s_2 and s_3 , then the set of all points corresponding to the polarized light form a sphere of radius 1, which is called the Poincaré sphere, figure 1.

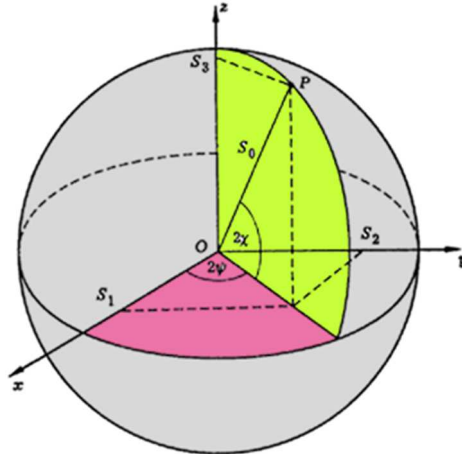


Figure 1. Poincaré sphere.

The condition of partially polarized light is represented by a vector of length SOP inside the Poincaré sphere. To unpolarized light $SOP = 0$, there corresponds the point of the beginning of coordinates.

The Stokes parameters allow to define conditions of polarization is non-uniform the polarized monochromatic light beam.

3. The model of the real-time differential polarimeter

The basis of our model is the task: to create the differential polarimeter allowing to define and investigate distribution of polarization it is non-uniform the polarized monochromatic light fields in real time.

The object is achieved in that the device for determining and investigating the polarization distribution, figure 2, comprising a $He-Ne$ laser, quarter wave plates and polarizers arranged perpendicularly to the radiation propagation path, the recording device is a CCD camera, contains a compensator configured as a diffraction grating arranged in parallel quarter wave plates and polarizers and perpendicular to the optical axis of the monochromatic light beam.

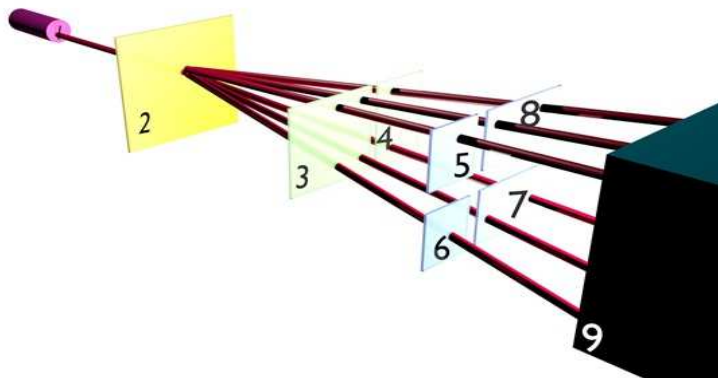


Figure 2. Experimental setup differential real-time polarimeter.

The device comprises, figure 2, a helium-neon laser (1), in the radiation path of which a compensator made in the form of a diffraction grating (2) is located, quarter wave plates (3), (4), polarizers (5), (6), (7), (8) located perpendicular to the optical axis of the beam, the recording device is a CCD camera (9). Diffraction grating, quarter wave plates, polarizers and camera are arranged parallel to each other.

To determine the polarization by the Stokes polarimetry method, six patterns of beam intensity distribution are measured in real time: two of which are linearly polarized along the axes x (I_x) and y (I_y), two are circularly polarized - right (I_r) and left (I_l) and two with mixed polarizations, at an angle 45° for (I_{45}) and -45° for (I_{-45}) axis x . Further, the light beam is recorded by the CCD camera, the image is transmitted to a personal computer. This device makes it possible to determine and investigate the polarization distribution of inhomogeneously polarized monochromatic light fields, in real time.

References:

- [1] R. Azuma 1997 *Survey of Augmented Reality Teleoperators and Virtual Environments*; pp.355-385
- [2] Brian X. Chen 2009 *If You're Not Seeing Data, You're Not Seeing*
- [3] M. Born, E. Wolf 1973 *Principles of Optics Science*; p.720
- [4] T.A. Fadeyeva, A.V. Volyar 2004 *Differential Polarimeter* №65939

The study of compacted singular beam transmitted in few-mode fiber

A A Ilyasova¹, S I Halilov¹, B V Sokolenko¹, A F Rubass¹

¹*V.I. Vernadsky Crimean Federal University, Vernadsky Prospekt, 4, Simferopol, 295007, Russian Federation*

Abstract. Currently popular and relevant challenge is the need to increase the capacity of existing fiber-optical communication lines. For solution of this problem proposed to use optical vortices, rather than the standard Gaussian beams. Due to its properties of optical vortices significantly increase the number of channels in the fiber, since the propagation in the fiber from the spin-orbit interaction, have a different propagation constant. The proposed method allows to increase the number of channels for information transmission in the fiber. It was found that in the radiation field, at the exit from the optical fiber, there are C-points, each of which corresponds to the polarization of the beams at the input. The topological index of the C-points corresponds to the charge of the original beams.

1. Introduction

Currently, the volume of data traffic through the Internet reaches its limits, due to fiber optic nonlinear effects. One of the urgent tasks is to increase the capacity of existing fiber-optic communication lines. One of the ways is the application of technologies for multiplexing and demultiplexing signals. Earlier, in this method, Gaussian beams were used to modernize the system. We used Laguerre-Gauss beams, also called optical vortices, which, due to their properties, significantly increase the number of channels in the fiber. The transmission of information in a fiber with the help of such beams is one of the most promising technologies for increasing the data transmission speed. It is known that the radiation field of a few-mode optical fiber typically contains the points of singularity, the position of which depends on the excitation conditions, external disturbances and the orientation of the polarizer. The only way to analyze processes in the fiber is the study of the radiation field of this fiber.

The aim of this work is to investigate experimentally the possibility of multiplexing and complex signal carrying optical vortices in few-mode optical fiber.

In this paper, the formation of an optical vortex was used a dielectric wedge. The process of the birth of an optical vortex is quite simple. This requires that the usual Gaussian beam falling on the surface of the transparent dielectric wedge so that one half passes through free space and the other through the wedge.

2. Model and results

The principle of the study is as follows (figure 1): after the division of the linearly polarized signal into two, having different state of polarization and a different sign of the topological charge, to multiplex the signal. And the output fiber, analyzing the superposition of the beams on the composition of the mod, we can distinguish the input signal. The difference beams in orbital angular moments is carried out interferometric methods. The difference beams as fields possible in the measurement of polarization States using a polarizing filter. In the fiber due to spin - orbit interaction angular momentum beams, the state of the topological charges of optical vortices and polarization state of the beams that are mixed. To determine the main polarization processes occurring in the fiber, we used a differential Stokes - polarimeter that allows measurement of the distribution division of the state of polarization of the radiation in each pixel of the image and output the corresponding map on the computer display.

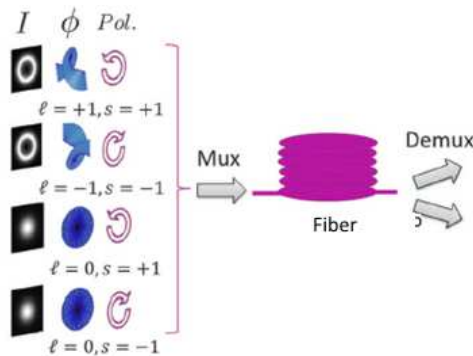


Figure 1. The spin transformation $s=\pm 1$ is realized with a quarter-wave plate.

For the study of process of multiplexing the signal in the fiber were collected, the experimental setup is depicted in figure 2.

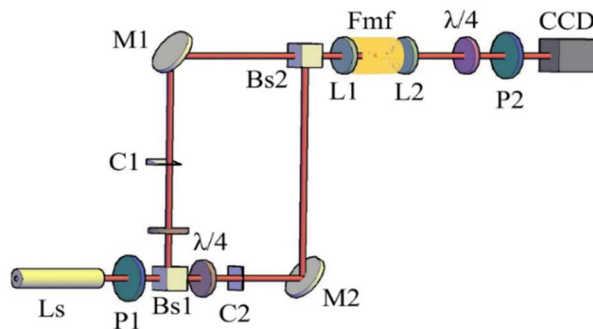


Figure 2. Schematic of the experimental setup: (Ls) Laser, (P) polarizer, ($\lambda/4$) quarter-wave plate, (Bs) beam splitter, (L) lens, (M) mirror, (C) dielectric wedge, (Fmf) few-mode fiber ($V = 3.4$), (CCD) camera.

A linearly polarized beam of He-Ne (Ls1) laser with a wavelength $\lambda = 0.6328\text{mkm}$, passing through the dividing cube (Bs1), is divided into two beams. Each of the beams of Gauss passes through the dielectric wedge (C1 and C2) and is diffracted, giving rise to optical vortices. Data generation method of an optical vortex was used in connection with the ease of implementation and great energy efficiency, which is important for excitation of optical fibers. Next to get a non-uniformly polarised radiation beam both pass through the polarizers (P1 and P2) and a composite phase plate ($\lambda/4$), configured so that when passing the plate radiation acquired circular polarisation of opposite signs. Then bring the two beam dividing cube polarizing filter (Bs2), thus multiplexing bundles in few-mode fiber. After passing through the fiber is measured the polarization States of the data beams by the method of Stokes-polarimetry. Results captures CCD camera. The data from the camera arrived on the monitor and on the computer where recorded and processed on a program of Differential polarimeter.

Figure 3 shows the intensity of the first and second beam separately, and the total intensity of the two orthogonal beams. In accordance with the classification of the Nai in our case, they correspond to singularities of the type "star" and "lemon". Knowing the polarization pattern after the fibre, we can analyze the modal structure of the radiation field and the composition of the input signal in the fiber.

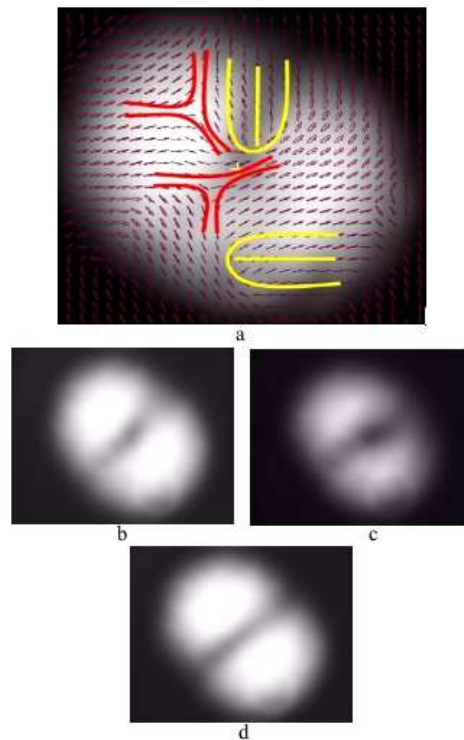


Figure 3. a) Map of the polarization states of beams having orthogonal polarization; b, c) The intensity distribution of the first, second beam; d) Distribution of the intensity of the total beam;

Thus, knowing the polarization pattern after the fiber, we can analyze the mode composition of the radiation field and the signal composition at the input to the fiber.

3. Conclusion

The proposed method allows to increase the capacity of existing fiber-optic communication lines. In the course of the work, the process of multiplexing Laguerre-Gauss beams into an optical low-mode fiber, produced by beams with different topological charges and different polarizations, was experimentally investigated. It is found that in the radiation field, at the exit from the few-mode optical fiber, there are C-points, each of which corresponds to the polarization of the beams at the input. The topological index of the C-points corresponds to the charge of the original beams.

References:

- [1] Shvedov V, Izdebskaya Ya, Alekseev A and Volyar A 2002 The Formation of Optical Vortices in the Course of Light Diffraction on a Dielectric Wedge, *Technical Physics Letters*, Vol. 28, No.3, pp.256–259
- [2] Berry M. Singularities in waves and rays // *Physics of defects. Les Houches Session XXXV*. Amsterdam: North-Holland. 1980. P.453-543.
- [3] Bazhenov V.Yu., Soskin M.S., Vasnetsov M.V. Screw dislocations in light wavefronts // *Journ. of modern optics*. 1992. V.39. No.5. P.985-990.

Simultaneous assessment of blood flow rhythmic oscillation by using of laser Doppler flowmetry and videocapillaroscopy methods

I.O. Kozlov¹, M.V. Volkov², I.P. Gurov², N.B. Margaryants², A.V. Potemkin², E.A. Zherebtsov³, V.V. Dremin¹, A.V. Dunaev¹

¹*Orel State University named after I.S. Turgenev, Orel, Russia*

²*ITMO University, Saint-Petersburg, Russia*

³*Aston University, Aston, UK*

Videocapillaroscopy is well-known method for evaluate of microvascular abnormalities such as Raynaud phenomenon and system sclerosis. This method is based on registration of frames series representing capillary blood flow and capillary forms. Other method that widely used for blood flow analysis is Laser Doppler Flowmetry (LDF). The main phenomenon in this technique is registration of laser radiation back-scattered from moving red blood cells. Recorded and digitized photocurrent is processed and after necessary computing operations we received index of microcirculation (Im.) This parameter is proportional to red blood cells velocity and concentration in diagnostic volume (1-3 mm³).

As index of microcirculation depends from blood dynamic in microvasculature, the graph of Im contains biological rhythms (endothelial, neurogenic, myogenic, breath, heart). A special interest for diagnostics can be the wavelet analysis of these oscillations during functional tests (occlusion, temperature, etc). The significant changes in the registered spectra usually can be associated with microcirculation insufficiency occurring with various rheumatic and endocrine syndromes.

Today, there are many doubts that LDF method can provide diagnostic information about blood flow oscillations and rhythms. In this research, we performed an objective comparison between the integral evaluation of blood flow by LDF and the single-capillary estimation by VCS.

The possibility to calculate the blood flow velocity in a single capillary was realised by the video capillaroscopic method. The in-house custom build setup consists of optical subsystem, high-speed IDS UI3060-CP camera and side illumination subsystem. In the system, the registered sequences of frames with a frame rate of 200 fps are processing by the novel dedicated algorithm.

A custom developed laser Doppler measuring channel supplemented by the dedicated software was used for the registration of perfusion. The signal processing model was implemented in the NI LabVIEW environment to calculate the index of microcirculation. The NI USB 6211 data acquisition board was used to digitise the received signal. Morlet wavelet transformation is used to calculate the spectra of registered signals.

A series of parallel 10-minute experimental records of the microcirculation index and videocapillaroscopic measurements were conducted.

The proposed approach demonstrated the essential correlation between spectra oscillations in the isolated capillary and the integral estimation of the microcirculation index by the laser Doppler flowmetry method. This result demonstrates the deep connection of the LDF signal with objective physical characteristics of the skin blood microflow.

Design and implementation of wavefront aberration correction by liquid crystal spatial light modulator

Xu Ning¹, Fu Yuegang¹, Pu Dong¹

¹School of Opto-Electronic Engineering, Changchun University of Science and Technology, Changchun 130022, China

In view of the aberration of optical system, a wave aberration correction based on liquid crystal spatial light modulator is proposed. As to approximate infinity imaging, digital wave-front phase-shifting interferometer is used for accurately measuring the wave-front of an optical system, thus obtaining the wave-front data matrix; as to finite focus distance, using Zemax simulation to obtain wave-front data matrix. In Matlab, use the data matrix to compile aberration fitting program and create corresponding 8-bit conjugate gray-scale image in BMP format. According to the phase modulation principle of liquid crystal spatial light modulator, load conjugate gray-scale image and wave-front distortion image of the modulator on the silicon based LCD panel, Imaging resolution is 1348LW/PH and above does not load the gray-scale is 337.8LW/PH. The test shows that: Imaging quality of photographic systems can be notably enhanced by loading conjugate gray-scale images of wave-front data.

Keywords:

Liquid crystal spatial light modulator; wave aberration correction; wave-front measurement; resolution.

Influence of silicon resonant particles on the surface plasmon-polaritons excitation efficiency

L N Dvoretckaia¹, A M Mozharov¹, A A Bogdanov^{1,2}, and I S Mukhin^{1,2}

¹ St. Petersburg Academic University, Khlopina 8/3, 194021 St. Petersburg, Russia

² ITMO University, 197101 St. Petersburg, Russia

E-mail: liliyabutler@gmail.com

Abstract. It is believed that optoelectronic processors will allow to operate large data streams without increasing power consumption, one of the possible ways of making such processors is based on developing the plasmonic nanoantennas excited by a tunnel current (1). Plasmonic nanoantennas excited by a tunnel current can be used to efficiently excite surface electromagnetic waves. However, dielectric nanoantennas have a magneto-dipole resonance in contrast to the plasmonic nanoantennas, since scattering electromagnetic waves by free charge carriers in plasmonic antennas and thus absorbing them (2). Using the silicon submicron particles having electric and magnetic dipole resonance effectively controlling the radiation is possible (3). In this paper numerical simulation of the plasmon propagation efficiency over a metal surface from a point dipole source with using a silicon particles will be presented. The results can later be used to develop optoelectronic processors.

1. Introduction

It is known that processors based on integrated microcircuits gradually reach the limit of their performance. Companies that manufacture processors for computing machines conduct research and develop methods for integrating optoelectronic data transmission systems inside processors (4). Such processors will allow processing large data streams without increasing power consumption.

To create optoelectronic processors it is necessary to develop a highly efficient radiation source compatible with silicon technologies. The source can be represented as radiation from inelastically scattered electrons in the tunnel gap. Such a gap can be created in the laboratory between the STM probe and the particle on the substrate. At the same time, the process of converting the electromagnetic wave of a source into a surface plasmon is of interest. This system will be investigated in this work. The process of formatting the surface plasmon can be made more efficient by using dielectric nanoantennas. To study the process of radiation capture in a surface plasmon it is necessary to study the interaction of radiation from a point source with silicon resonating particles on a metallic waveguide. In this paper numerical simulation of the plasmon propagation efficiency over a metal surface from a point dipole source using silicon submicron particles as an element that enhances the intermode transformation of radiation will be presented.

2. The modelling

In numerical simulation the radiation source is represented as a point dipole. The source acts on a silicon nanoparticle in the form of a sphere with a diameter of 50-300 nm which is located on a gold substrate. We analyze the result of acting the source on a particle at which arise a plasmon-polariton propagates along a metal waveguide. In this paper the dependence of the conversion efficiency of the

electromagnetic wave of the source to the plasmon-polariton mode on the nanoparticle diameter will be presented.

3. Conclusion

As a result of the work done a numerical model of the source of the optoelectronic device was constructed. It is shown that the efficiency of converting the electromagnetic energy of a source into a surface plasmon-polariton depends on the diameter of the nanosphere. In the following we will consider the effect of the tip of the tunnelling microscope on the excitation efficiency of the SPP.

References:

- [1] Koenderink A F, Alù A and Polman A 2015 *Science*, 348(6234), pp.516-521
- [2] Sinev I S, Bogdanov A A, Komissarenko F E, Frizyuk K S, Petrov M I, Mukhin I S, Makarov S V, Samusev A K, Lavrinenko A V and Iorsh I V 2017 arXiv preprint arXiv:1705.07689
- [3] Schmidt M K, Esteban R, Sáenz J, Suárez-Lacalle I, Mackowski S and Aizpurua J 2012 *Optics express*, 20(13), pp 13636-13650
- [4] Desmulliez M P 2000 *Materials Science and Engineering B* 74(1), pp 269-275

An optimized design of miniaturized terahertz time-domain spectrometer

Shijia Feng¹, Ming Liu¹, Yuejin Zhao¹, Zhuo Li¹, Xiaohua Liu¹, Liquan Dong¹, Hong Wu¹

¹ Beijing Key Laboratory for Precision Optoelectronic Measurement Instrument and Technology, School of Optoelectronics, Beijing Institute of Technology, Beijing 100081, China

A miniaturized terahertz time-domain spectrometer is designed and optimized. The titanium sapphire laser is adopted as the laser source, and the terahertz pulses are generated through the gallium arsenide photoconductive antenna and detected with zinc telluride crystals. Specially, by using the internal focusing microscope, the generation and detection optical beam path is precisely aligned and the precision is largely improved. Compared to the design of the traditional terahertz time-domain spectroscopy system, the instrument volume is reduced and the adjustment difficulty is reduced. The volume of the spectrometer changed from the previous 640mmX460mmX386mm to the improved 470mmX280mmX150mm. Finally, the prototype is tested. The results show that the spectral range is 0.1~4THZ, the scanning range is more than 150mm, and the corresponding spectral resolution is less than 5GHz.

Modeling of self-consistent modes in optical fibers with $V=3.8$

S Halilov¹, Y Akimova¹, A Ibragimov¹, A Rubass¹, A Ilyasova¹, B Sokolenko^{1,2}

¹ Physical-Technical Institute, V.I. Vernadsky Crimean Federal University. Simferopol, 295007, Russia

² Department of Science and Research, V.I. Vernadsky Crimean Federal University. Simferopol, 295007, Russia

Abstract. The results of modeling the intensity and polarization distribution of both its own and the combination mode of the composition of the isotropic fiber with a gradient a refractive index profile having a waveguide parameter $V=3.8$.

1. Introduction

The main problem of the current fiber-optic communication is low bandwidth. To increase the number of channels in the fiber, the authors [1] used a singular beams. Such beams possess an additional third degree of freedom to increase the number of channels in fiber - orbital angular momentum [2], which does not depend on the polarization state and the wavelength of the radiation beam. To summarize and transmit information along the fiber using singular beam, it is necessary that the waveguide fiber were greater than 2.4. Based on the solutions of the characteristic equation, when a waveguide parameter $V=3.8$ implemented 12 mod that can carry the singularity. Therefore, the aim of this work was to simulate the self-field vector distribution and polarized low-mode optical fiber with $V=3.8$, and combinations thereof.

2. The construction of intensity and vector distribution of the polarization field of the fiber.

Consider the theoretical description of the construction of (a) intensity and (b) polarization patterns for fashion LP_{11} .

(a) The field LP_{11} is of mode combination is obtained by adding HE_{21} and TM_{01} or TE_{01} mod. Even the x-polarized input LP_{11} fashion has the following form:

$$E_x = F_1(R) \cos \varphi \cos(\delta\beta_{21}z) \exp(i\tilde{\beta}z) \quad E_y = iF_1(R) \sin \varphi \sin(\delta\beta_{21}z) \exp(i\tilde{\beta}z) \quad (1)$$

where $\delta\beta_{21}$ is half-difference propagation constants HE_{21} and TM_{01} , $\tilde{\beta}$ -sum propagation constants HE_{21} and TM_{01} mod, to simplify the description of the radial functions used the approximation of a parabolic refractive index profile, then

$$F_1(R) = R^l \exp\left(-\frac{VR^2}{2}\right)$$

where $R = r / \rho$, $\tilde{\beta} = kn_{co} \left\{ 1 - \frac{4\Delta}{V} (2 + l - 1) \right\}$, $m=1$, $l=1$

The intensity distribution in the case of a vector field is equal to zero Stokes parameters: $I \equiv S_0 = |E_x|^2 + |E_e|^2$. Since the basic object-oriented programming languages there is no complete support for complex numbers, the field is conveniently split into real and imaginary parts. For the field LP_{11} of fashion:

$$\begin{aligned}
 E_{xr} &= F_1(R) \cos \phi \cos(\delta\beta_{21}z), & E_{yr} &= 0, \\
 E_{xi} &= 0, & E_{yi} &= F_1(R) \sin \phi \sin(\delta\beta_{21}z).
 \end{aligned}$$

Then the intensity can be represented as:

$$I = S_0 = |E_x|^2 + |E_y|^2 = E_{xr}^2 + E_{xi}^2 + E_{yr}^2 + E_{yi}^2$$

(b) According to formula (1), the LP_{11} mode combination at each point of cross-section in the fiber is fully polarized. In the General case of an arbitrary point in the Le has an elliptical polarization. As is known, the polarization is characterized by the following parameters: the intensity I, degree of ellipticity of Q and the tilt angle ψ , the greater semi-axis to the x axis of the laboratory coordinate system. The degree of ellipticity is defined as $Q = \pm b/a$, where the sign "+" is taken if the electric vector rotates clockwise in the plane of observation (light got). These parameters are uniquely determined by the Stokes parameters

$$I = S_0,$$

$$\psi = \frac{1}{2} \arctan\left(\frac{S_2}{S_1}\right),$$

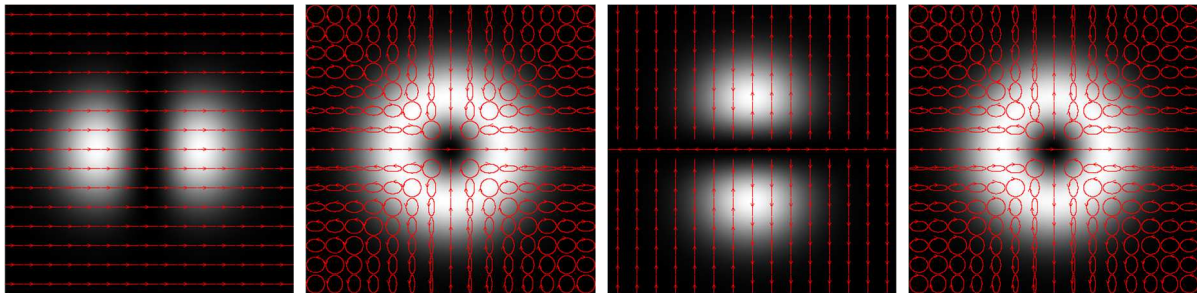
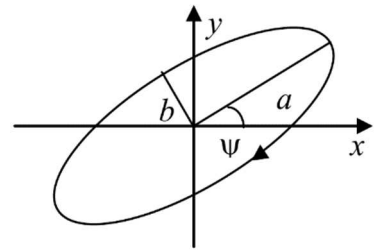
$$Q = \tan\left(\frac{1}{2} \arcsin\left(\frac{S_3}{S_0}\right)\right)$$

where: $S_0 = |E_x|^2 + |E_y|^2 = E_{xr}^2 + E_{xi}^2 + E_{yr}^2 + E_{yi}^2,$

$$S_1 = |E_x|^2 - |E_y|^2 = E_{xr}^2 + E_{xi}^2 - E_{yr}^2 + E_{yi}^2,$$

$$S_2 = E_x^* E_y + E_x E_y^* = 2(E_{xr} E_{yr} + E_{xi} E_{yi}),$$

$$S_3 = i(E_x^* E_y - E_x E_y^*) = 2(E_{xr} E_{yi} - E_{xi} E_{yr})$$



(a)

(b)

(c)

(d)

Figure 1. The distribution of polarization LP_{11} fashion, at $\lambda=650$ nm., $r=3.5$ μm ., $z=0$ cm (a), 45 cm (b), 90 cm (c), 135 cm (d).

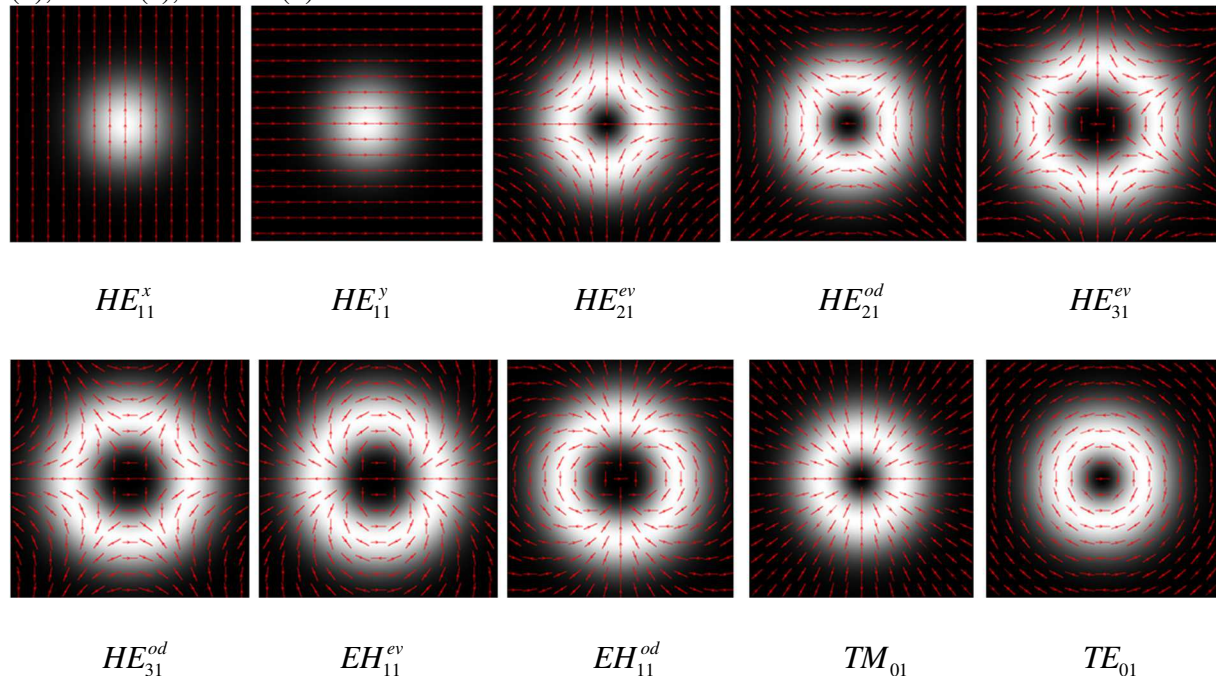


Figure 2. Own fashion fiber with $V=3.8$ at $\lambda=650$ nm., $r_1=5$ μm ., $r_2=3.5$ μm ., $z=0$ cm.

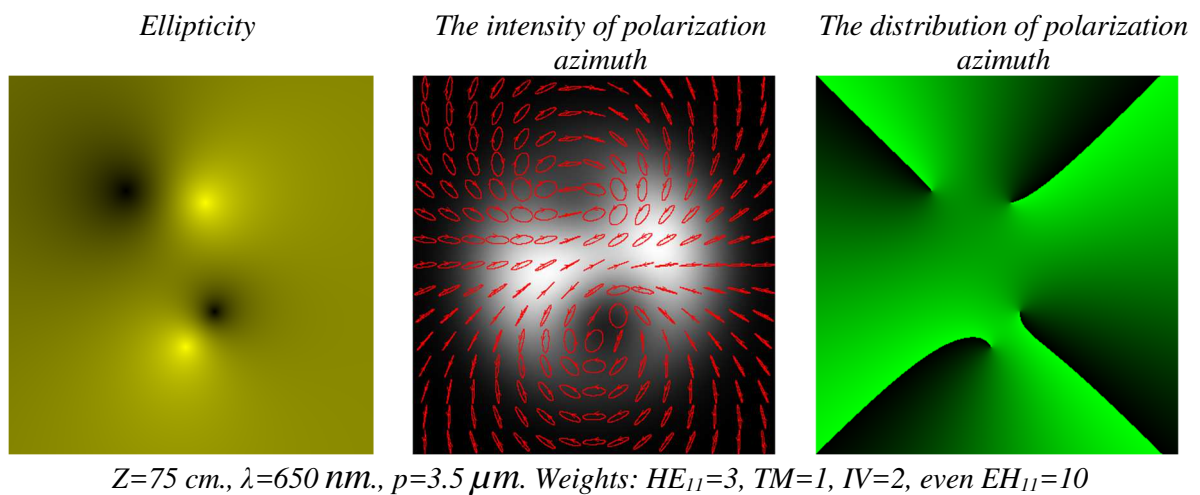


Figure 3. The superposition of the natural modes of the fiber

3. Conclusion

In the result, a program was written for simulating basic fashion as well as all possible combinations of the mode composition of propagating in an isotropic fiber with a gradient index profile having a waveguide parameter $V=3.8$. The program allows you to build a distribution of polarization, the ellipticity and azimuth for the complex modal combinations.

References:

- [1] Nenad Bozinovic, Yang Yue, Yongxiong Ren, Moshe Tur, Poul Kristensen, Hao Huang, Alan E. Willner, Terabit-Scale Orbital Angular Momentum Mode Division Multiplexing in Fibers // Science, 2013.
- [2] Nye J.F., Berry M.V., Dislocations in wave trains // Proc. R. Soc. Lond. A. – 1974. – V.336. – P.165 - 190.

Free Space OTDM System based on Pulse Width Compression of Supercontinuum

Junda Chen¹, Xinmeng Zhang¹, Peng Lin¹, Ziqi Jiang¹, Chengbo Wang¹ and Tianshu Wang¹

¹ National and Local Joint Engineering Research Center of Space Optoelectronics Technology, Changchun University of Science and Technology, Changchun 130022, China

E-mail: wangts@cust.edu.cn

In this paper, an optical time division multiplexing communication(OTDM) scheme which is based on a pulsed light source with supercontinuum is proposed. A pulse with narrower pulse width can be formed when laser pulse pumped into high non-linear fiber(HNLF) because of non-linear effect. We initially set up a communication link with a bit rate of 200Mbit/s while the pulse width is compressed more than 60%. Owing to the extensive spectrum bandwidth of free space optical communication, this scheme can become a new idea to increase the speed rate of free space optical communication.

Keywords:

Time Division Multiplexing, Free Space Optical Communication, Pulse Width Compression, Supercontinuum

Generation of microwave vortex field

D Poletaev¹, B Sokolenko²

¹*Department of radiophysics and electronics V.I. Vernadsky crimean federal university, Simferopol, Russia*

²*Department of general physics V.I. Vernadsky crimean federal university, Simferopol, Russia*

E-mail: poletaevda@cfuv.ru

Abstract. In this paper a method for the formation of microwave vortex field is proposed. A numerical simulation based on the finite element method is conducted. The conducted research confirms the possibility of the formation of a vortex field microwave near the open end of the circular waveguide. The calculations yielded a picture of the field distribution in the near and far zones.

1. Introduction

The vortex of space-time structure is typical for many physical processes. At the present time the attention of researchers working in the field of laser physics and coherent optics, attracted to field of light with helical perturbations of the wave front. Such perturbations are responsible for the propagation of a vortex of light energy – optical vortices. These physical phenomena are successfully used for the manipulation of micro- and nano-objects, the implementation of long-distance communications, sensing of the atmosphere and objects [1, 2]. Microwave electromagnetic waves are very similar to the light. It may be characterized by the Poynting vector and angular momentum.

There are a number of articles that tell about the successful formation of the vortex field microwave [3, 4]. So one of them used a spiral antenna, which allows to provide the necessary deformation of the wavefront. However, a disadvantage of this method is the inability to obtain significant power of the vortex field. It seems reasonable to propose a method for the generation of microwave vortex field.

The purpose of this paper is the analysis and numerical simulation of the formation of microwave vortex field near open end of the circular waveguide.

2. Theoretical part and simulation results

2.1. Theoretical data

In the microwave technique is widely used circular waveguide. The most interesting from a physical point of view, in terms of the application for the formation of optical vortices is type H₀₁ of magnetic wave. The main advantage of it is the low ohmic losses, due to only radial currents in the waveguide [5]. However, there are certain difficulties in excitation and isolation of this wave type in the waveguide. Electric power lines H₀₁ wave in a circular waveguide are a closed circle. Open end of the circular waveguide with this type of wave radiates into free space is the simplest antenna. Obviously, this method is not without drawbacks. However, at this stage analyze the possibility of formation of the vortex field, using a circular waveguide.

Building a model based on the general theory of the electromagnetic field and the apparatus of mathematical physics, in particular, the finite element method. In this case, the model space is divided into tetrahedra, values of the electric and magnetic fields are calculated at the vertices [6]. To establish

the existence of microwave vortex field is convenient to use directional patterns. They allow to get a complete picture of the field distribution in space.

The numerical modeling of radiation from a circular waveguide with a radius of 19.3 mm at 10 GHz, allowed to build the following directional patterns in the near field zone (20 mm) and far field zone (at infinity) (fig. 1).

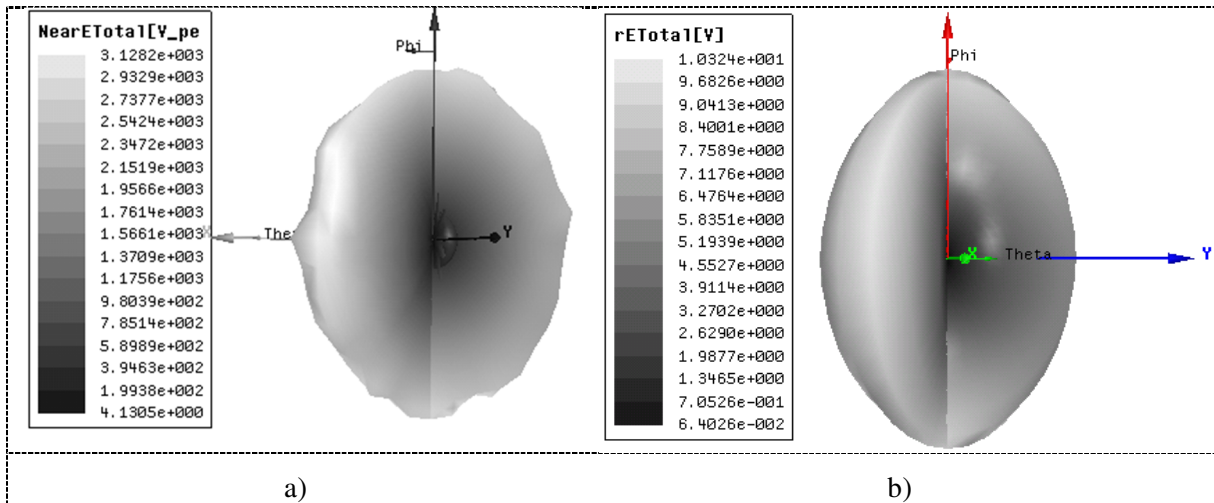


Fig. 1. Directional patterns from a circular waveguide a) the near field (20 mm), b) the far field (at infinity)

As can be seen from the graphs (fig. 1), the radiation of wave type H01 from the open end of circular waveguide is not a vortex. Heterogeneity is required to produce the phase shift. Heterogeneity may be a dielectric with the relative permittivity $\epsilon > 1$. Empirically, the following structure as a half of a truncated cone with $\epsilon = 5.5$ was chosen (fig. 2). It allows optimal align the wave impedance of the waveguide and free space.

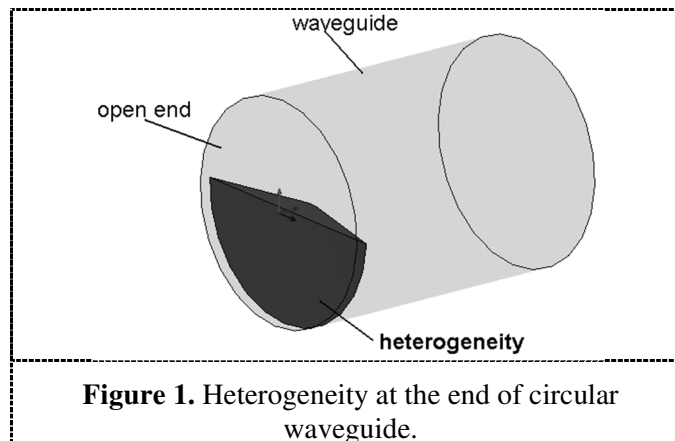


Figure 1. Heterogeneity at the end of circular waveguide.

This heterogeneity makes it possible to shift the phase of the electric field vector, and introduce some screw dislocation in the field. Numerical simulation of circular waveguide with a radius of 19.3 mm and a half of a truncated cone with $\varepsilon = 5.5$ at the end of the frequency of 10 GHz, allowed to build the following pattern in the near field zone (20 mm) and far field zone (at infinity) (fig. 3).

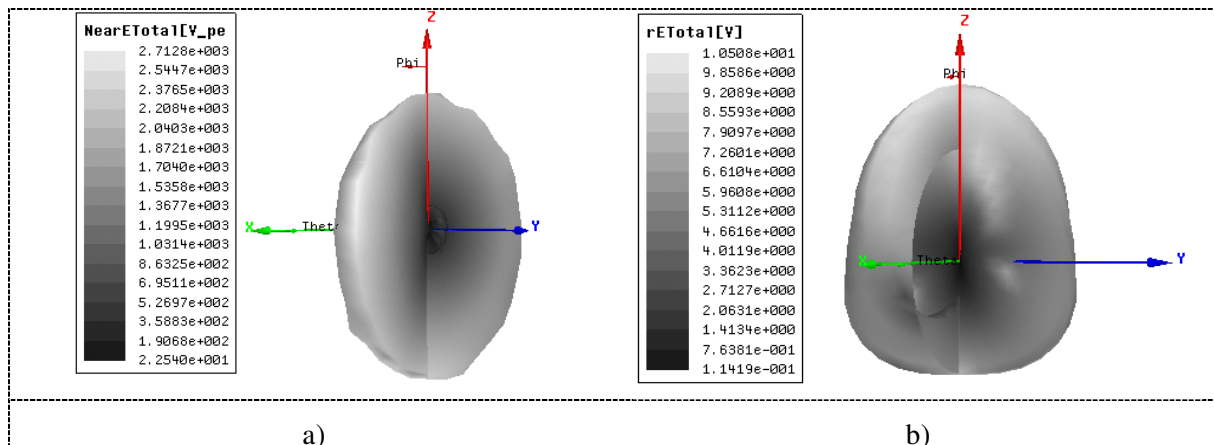


Fig. 3. Directional patterns from a circular waveguide with a half of a truncated cone at the end of a) the near field (20 mm), b) the far field (at infinity).

As can be seen from the diagrams (fig. 3), this structure can form a vortex field in the far zone. Directional pattern (fig. 3, b) is a spiral, which confirms the presence of a vortex field. Phase of the electric field changes not only in the time, but also in space.

3. Results and Discussion

The numerical simulation confirms the possibility of the formation of microwave vortex field near open end of the circular waveguide. The calculations allowed to establish a field distribution in the near and far zones.

References:

- [1] Korolenko P.V Optical vortices 1998 *Soros Educational Journal* **6** 133-143.
- [2] Fadeyeva T.A *et al* The vortex-beam precession in a rotating uniaxial crystal 2009 *J. Opt. Appl.* **11** 343-354.
- [3] Fabrizio T 2012 Encoding many channels on the same frequency through radio vorticity: first experimental test *New J. Phys.* **14** 120-134.
- [4] Chen L, Ong C, Neo C 2004 *Microwave electronics measurement and materials characterization* (New York: John Wiley & Sons) pp 123-130.
- [5] Itoh T 1989 *Numerical techniques for microwave and millimeter-wave passive structures* (New York: John Wiley & Sons) pp 333-35.

Optical vortex profilometry with nanoscale resolution

B Sokolenko¹, D Poletaev², N Volockaya³, S Halilov¹, A Ilyasova¹, A Prisyazhnuk¹

¹ *General Physics department, Institute of Physics and Technology of V I Vernadsky Crimean Federal University, Vernadsky Av, 4, Simferopol, 295007, Russia*

² *Radiophysics and Electronics department, Institute of Physics and Technology of V I Vernadsky Crimean Federal University, Vernadsky Av, 4, Simferopol, 295007, Russia*

³ *Medical Academy named after S.I. Georgievsky, V I Vernadsky Crimean Federal University, Vernadsky Av, 4, Simferopol, 295007, Russia*

Abstract. Practical application of optical vortex in a method of three-dimensional profilometry with nanoscale resolution was considered. It was shown that phase analysis of coherent light beam carrying axial optical vortex allow to retrieve information about sample surface relief. High spatial resolution caused by vortex helical phase sensitivity to disturbances in wave front after reflection or spreading through studying sample, which can be optically transparent or have a reflecting surface. This method applicable for non-destructive testing of live cells and biological tissues in real-time regime with exceeding optical diffraction limit. Computer processing of vortex interferograms allow to achieve a vertical resolution down to 1,75 nm. Specially designed optical scheme reduces an environment influence, in particular, vibration, misalignment of test sample and its local anisotropy and provides the possibility of investigating surfaces of large linear dimensions. The prospective tasks of automated systems creation for monitoring of surface quality were proposed, in particular those that will could be developed with methods based on singular optics and phase singularities.

1. Introduction

The unique properties of optics of singular beams that are able to transform a Gaussian beam into a vortex one, control and observe its parameters find a use in different devices for trapping, transportation, and angular orientation of microparticles [1]. Last significant research effort has been invested in its physical implications and possible applications of vortex beams, especially in microscopy, profilometry and digital imaging. There are a great number of articles devoted to the problem of a beam reflecting or transmitting through the observable sample in both coherent and non-coherent light [2] for non-contact metrology of nanostructures. Such techniques can be used for controlling of surface profile in various fields of technology, in the debugging of technological processes and in express testing of the final product and in scientific research [3].

In the present research we focus our attention on the interferometric analysis of phase evolution of light beam carrying optical vortex and its application to profilometry. This technique is able to perform measurements of thickness and surface topology without direct contact with an object in non-destructive way with high accuracy. A well-known practical application of optical vortex in the vortex scanning optical imaging allows to study, for example, the surface geometry and optical density of the sample by analysis of phase singularity's distortion. Also, it was shown that vortex phase analysis carrier information about topology of surface, and depends of the features of incident beam and different aperture of optical systems [4]. In manuscripts [5, 6] authors developed a new solution called Optical Vortex Scanning microscope where the sample is scanned by moving vortex lens producing a vortex movement inside the beam by characteristic way. This study demonstrates the response of the optical vortex imbedded in focused Gaussian beam to the phase steps inside the object arm of interferometer. Scanning of sample enables to plot a vortex trajectory, which has a different inclination angles to the direction of vortex lens movement and depends on thickness of the probe. Further research of Optical Vortex Scanning Microscope conducted with developing of analytical models and phase retrieval algorithms [7]. The last investigation [8] describe both theoretical and experimental results of imaging

system using movable optical vortex, where the image of the probe was combined with the structure of the vortex beam.

Nevertheless, the phase distribution after the object may recovered with quite good accuracy, thus the model of the Optical Vortex Scanning Microscope opens new possibilities for the development of reconstruction procedures and for optical system optimization.

The main difficulties of methods, which uses an interferometry and coherent light sources, are very high sensitivity to vibration and axial alignment as well as speckle noise.

In this paper we consider analytically and experimentally optical scheme of three-dimensional optical profilometer with nanoscale resolution using the monochromatic linearly polarized along x-axis beam carrying single-charged optical vortex with the wavelength λ and transmitting through the isotropic glass plate with complex surface relief, which provokes additional phase transformations. By analysing of captured interference patterns in form of fringes and spiral line, we can extract an information about surface topology or sample thickness.

2. Optical vortex profilometry: the methodology

Let us consider the propagation of the paraxial beam along the z-axis. The transverse E_x component have a wavenumber $k_x = nk_o$, where k_o is a wavenumber in a free space and $n = \sqrt{\epsilon}$ – refractivity index of a test sample. In the paraxial approximation, we can treat the linearly polarised component as $E = \tilde{E}_x(x, y, z)\exp(-ik_x z)$. Then, the paraxial equations for the complex amplitude \tilde{E}_x can be represented in the form [29]:

$$d_x^2 \tilde{E}_x + d_y^2 \tilde{E}_x - 2ik_x d_z \tilde{E}_x = 0 \quad (1)$$

A particular solution to the paraxial wave equation (1) for the vortex beam we can write in the reference frame x, y, z of the sample:

$$\tilde{E}_x = \left(\frac{x - i\xi y}{w_o \sigma_o} \right) \times \exp\left[-(x^2 + y^2) / w_o^2 \sigma_o \right] / \sigma_o \quad (2)$$

where: $\sigma_o = \frac{1 - iz}{z_o}$, $z_o = \frac{nk_w^2}{2}$, w_o – is the radius of the beam waist at the sample plane ($z = 0$), $\xi = \pm 1$

– is the vortex topological charge. The vortex state is described by the equation $\text{Re} \tilde{E}_x(x, y, z) = \text{Im} \tilde{E}_x(x, y, z) = 0$. In such wise, the main parameters used in optical profilometer are: w_o – waist radius, Δz – geometrical path difference and $\Delta\varphi$ – phase difference caused by various thickness of explored sample and n – refractivity index for transparent materials.

The phase of singular beam is extremely sensitive to any changes in material parameters and surface relief, such as thickness, local protrusions and dents, as well as refractivity index of chosen substance. Therefore, this phenomenon can be exploited for metrology purposes with high resolution and allow to study different physical processes at the nanoscale.

The interference of singular beam in axial (a) and tilted beams (b) and its phase pattern (c) are shown in figure 1. The typical “fork” which is formed in tilted interfering beams depicts a vortex position on the one hand, while the phase pattern has a helical form on the other hand and can be extracted from interference fringes by method, used in research [4].

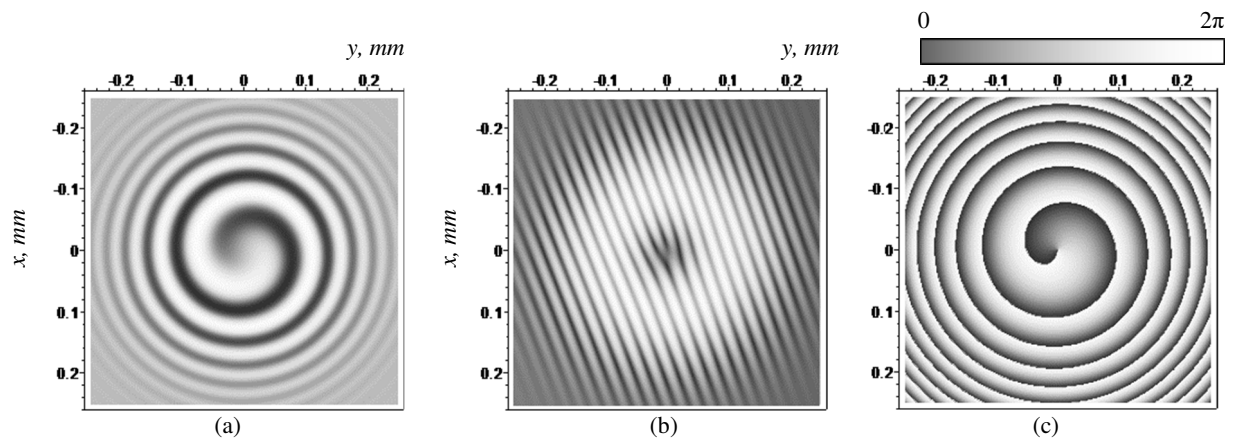


Figure 1. Calculated interference pattern of singular beam in axial (a) and tilted beams (b) and its phase pattern (c) with topological charge $\xi = +1$. Beam parameters are next: $\omega_0 = 70 \text{ } \mu\text{m}$, $n_x = 1.54$, $z = 20 \text{ mm}$, $\lambda = 632.8 \text{ nm}$.

As we can note from the figure 1, phase patterns of helical shape may show a rotation caused by optical path difference. Observable rotation is quite enough to distinguish step of 5 nm. Depicted pairs of interference and phase pictures illustrate the possibility to process not only clear phase of singular beam, but also directly the spiral produced by interference of singular and Gaussian beams after some adjustment of contrast and brightness. This method is applicable for fast and rough analysis of sample's shape.

3. Conclusion

In the present research we have theoretically and experimentally considered evaluation of singular beam's phase sensitivity and have shown that the distinguishable spiral phase rotation occurs at the isotropic plate thicknesses equals to $\lambda/120$, where λ – is a wavelength. Proposed technique may be applied to profilometry of optically transparent and reflecting surfaces with exceeding optical diffraction limit. Moreover, this method is applicable for non-destructive testing of live cells and biological tissues in real-time regime. Automatic processing of vortex spiral interferograms in conjunction with focusing unit will allow to achieve theoretically calculated limit of vertical resolution down to 1,75 nm for visible light and longitudinal resolution down to 7 nm. Another achievable technical result is the possibility to observe surfaces of substantially larger dimensions than other known profilometers allow, since the size of the surface under investigation is limited only by a specific implementation of the conjugation block used. This allows us to use the developed optical profilometer for non-contact measurements and metrological testing directly in industrial conditions.

References:

- [1] Molloy J E, Dholakia K and Padgett M J 2003 J. Mod. Opt. **50** 1501
- [2] Sprague R 1972 Applied Optics **11** 2811
- [3] Lukin E S, Anufrieva E V, Popova N A, Morozov B A, 2009 Functional Ceramics **1** 35
- [4] Popiołek-Masajada A, Sokolenko B, Augustyniak I, Masajada J, Kohoroshun A, Bacia M 2014 Opt. Lasers Eng. **55** 105
- [5] Masajada J, Leniec M, Augustyniak I 2011 J. Opt. **13** 03571
- [6] Augustyniak I, Popiołek-Masajada A, Masajada J, Drobczynski S 2012 Appl. Opt. **51** C117
- [7] Plociniczak Ł, Popiołek-Masajada A, Masajada J, Szatkowski M 2016 Appl. Opt. **55** B20
- [8] Popiołek-Masajada A, Masajada J, Kurzynowski P 2017 Photonics **4** 38

Holographic formation and properties of hybrid surface-relief/volume periodic structures

P.P. Sokolov¹, N.D. Vorzobova¹

¹ ITMO Univesity, St.Petersburg, Russia

Currently a large number of works have been devoted to the processes of forming three-dimensional structures and elements on their basis by various methods and in various materials. In this paper, the holographic process of forming three-dimensional structures based on photopolymeric materials is considered. In the literature, processes are mainly considered for the formation of three-dimensional structures with the refractive index modulation as a result of photo-initiated mass transfer in the interference field or processes of relief structures formation.

The objective of this work is to study the formation processes and properties of hybrid periodic structures. A hybrid periodic structure is a structure consisting of a volume grating with a modulation of the refractive index and a relief grating. The formation processes and properties of these structures have not been studied practically. The structures were formed by the holographic co-beams recording in photopolymerizable acrylate compositions.

Volume structures with modulation of the refractive index were formed between two surfaces. Hybrid structures were formed by removing the cover plating after exposure, as well as subsequent washing out of the unpolymerized material. On the basis of the dependence of the diffraction efficiency on the recording frequency and layer thickness the optimal conditions for the formation of volume structures with modulation of the refractive index were defined.

Further, on the basis of the investigation of the dependence of the diffraction efficiency of the hybrid structures on the exposure parameters, the conditions for the formation of surface gratings with the greatest depth of the relief are determined.

The contribution of the relief gratings to the diffraction properties of hybrid structures is determined. The selective properties of hybrid structures were studied. It was shown that the formation of a relief grating on the surface of volume grating leads to a change in the selective properties of the structures - an significant broadening of the angular selectivity contour with maintaining high diffraction efficiency over a wide range of angles of incidence.

For the first time, structures were obtained that combine the properties of volume and relief gratings with high characteristics that require for the practical problems. Possible applications of hybrid structures for the fabrication of protective elements and elements of solar concentrators are proposed.

Assessment of the influence of different concentrations of zinc on the brain biochemical processes in rat model

**O. Stelmashchuk¹, E. Seregina¹, G. Piavchenko¹, E. Vorobyev¹, E. Kuznetsova¹,
A. Alekseev¹, E. Zherebtsov², A. Dunaev¹**

¹ Orel State University named after I.S. Turgenev, Komsomolskaya b. 95, Oryol, 302026, Russia

² AIPT, Aston University, Aston Triangle, Birmingham, B4 7ET, UK

Being necessary for protein synthesis, zinc acts like a regulator, steering many important processes in enzyme systems in the right direction. Zinc compounds play important role in the controlling of muscle contractility, the insulin formation as well as in maintaining blood homeostasis and acid-base balance in the body. However, the zinc surplus has many pathological effects for organism.

Modern optical technologies show considerable advantages in application for drug discovery in small laboratory animals during efficiency and toxicity trials. In this study, using the fibre-optic probe, the fluorescence of the anterior brain regions was evaluated and analysed in a Wistar rat model. The probe made it possible to simultaneously record both fluorescence intensity and blood content parameters of the studied tissue site. To modulate the metabolic activity of brain tissues, Zn compound solution (in the form of zinc sulphate) of four different concentrations were administrated to the animals from treatment groups for 1 month in drinking water. After that, the fluorescence signals were measured on the brain cortex surface. Excitation at wavelengths of 365 nm, 450 nm, 532 nm and 637 nm was used to record the fluorescence signals. The processing of the obtained experimental spectra made it possible to reveal a direct relationship between the fluorescence intensity in the spectral region of NADH emission and the concentration of the orally administrated zinc. Optical measurements *in vivo* were supplemented by histochemical measurements of zinc ions in brain sections both in the treatment and control groups. The obtained results are in agreement with the statement that high concentrations of zinc ions are capable of inhibiting the mitochondrial complexes I, II and IV. The effect leads to inhibited cellular respiration in the cells of the nervous tissue.

It is well known that the activity of cortical neurons depends on the oxygen consumption in this cells. The dose dependent effect evaluation showed that the highest Zn concentration in dranked water caused intensity of the cell respiration. As a result in according with open field test the motor activity of the laboratory rats increased when low dose of Zn solution was added to water. Thus the concentration of Zn in water solution increased from 0.25 to 0.5 and then to 0.75 mg per animal it was noticed also the paradox effect that behavior of rats changed from aggressive (in low dose) to calm (in high dose). This may be explained as an effect of strong mitochondrial disfunction and pathological changes in the brain regions.

Demonstration of free space optical transmission in weak turbulence based on partially coherent sources in a novel method

Xinmeng Zhang,^{1,2} Junda Chen,^{1,2} Peng Lin,^{1,2} Zhiwen Sun,^{1,2} Chengbo Wang,^{1,2}
Tianshu Wang,^{1,2,*}

¹ National and Local Joint Engineering Research Center of Space Optoelectronics Technology, Changchun University of Science and Technology, Changchun 130022, China

² College of Opto-Electronic Engineering, Changchun University of Science and Technology, Changchun 130022, China

E-mail: wangts@cust.edu.cn

We design an experimental structure of free space optical transmission based on supercontinuum as a carrier. Based on properties for partially coherence of supercontinuum, we modulate and demodulate the partially coherent beams by the method of OOK in a turbulent channel and also measure the eye-diagrams, minimum sensitivity of 1Gbit/s, bit error rate (BER) and scintillations of coherent beams and partially coherent beams as a carrier respectively. By comparing the experimental results, it is obviously shown that lower minimum sensitivity which reaches -10dBm and lower intensity of scintillations can be obtained by means of free space optical transmission based on supercontinuum as a carrier. We experimentally demonstrate that it is feasible to construct a 1km link of free space optical transmission based on supercontinuum as a carrier.

Keywords:

Supercontinuum , Free Space Optical Communication, Atmospheric Turbulence

Study on Frequency Domain Characteristics Measurement of Pulse Signal in Atmosphere Laser Communication

Yao Haifeng¹, Ni Xiaolong¹, Tong Shoufeng¹, Liu Zhi³, Chen Chunyi², Jiang Huilin¹

¹ Institute of Space and Photoelectric, Changchun University of Science and Technology, Changchun, Jilin, 130022, China

² Electronic Information Engineering College, Changchun University of Science and Technology, Changchun, Jilin, 130022, China

³ Graduate School of Changchun University of Science and Technology, Changchun, Jilin, 130022, China

Atmospheric turbulence and Communication system device have great influence on the performance of the atmospheric laser communication system reducing the signal to noise ratio (SNR) and increasing the bit error rate (BER). In this paper, a spectral analyzing method is used to analyze the influence of atmospheric turbulence and operating noise and response characteristics of laser and detector on the signal. An experiment of laser beam propagation characteristic is carried out on a 6 km horizontal atmospheric link, and analysis the influence of atmospheric turbulence on the power spectral density of the rectangular pulse signal in different frequency ranges; optical path transmission experiment indoor, the influence of the operating noise and response characteristics of the laser and photodetector on the power spectral density of the rectangular pulse signal is analyzed. It is shown that: as the attenuation of atmospheric turbulence, when the rectangular pulse signal is transmitted through the atmospheric channel, the rectangular pulse power of the receiver is reduced in the whole frequency range; In the low frequency range, as the frequency of the signal in the frequency range of atmospheric turbulence (tens to hundreds of Hz) the power of the rectangular pulse signal in the receiver is reduced, however, due to the presence of communication system noise, the power of the rectangular pulse signal increases slightly in the frequency range of a few tens of Hz; In the 10^6 Hz frequency range, as the influence of the operating noise and response characteristics of the laser and photodetector, the power of the rectangular pulse signal is increased obviously, and form a “bulge”; the noise power increases in the high frequency range ($10^8\sim 10^9$ Hz).

A novel continuous-terahertz-wave molecular imaging method for biomedical applications

Rui Zhang¹, Shijia Feng¹, Liangliang Zhang², Shijing Zhang¹ and Yuejin Zhao¹

¹ Beijing Key Laboratory for Precision Optoelectronic Measurement Instrument and Technology, School of Optoelectronics, Beijing Institute of Technology, Beijing 100081, China

² Key Laboratory of Terahertz Optoelectronics, Ministry of Education, and Beijing Advanced Innovation Center for Imaging Technology, Department of Physics, Capital Normal University, Beijing 100048, China

Recently, terahertz (THz) imaging has been widely applied to distinguish lesions from normal tissues because THz radiation is non-ionizing and sensitive to water and to the motion of biological macro-molecules [1]. Furthermore, to improve image contrast between diseased and normal tissues, nanoparticle-enhanced THz molecular imaging techniques have been proposed and applied to cancer diagnosis and drug delivery detection [2-5]. Various nanoparticles, such as gold nanoparticles (AuNPs) or superparamagnetic iron oxide nanoparticles (SPIOs), were adopted as imaging probes. The main reason for signal amplification is that the power absorption and refractive index of water are temperature-dependent in the THz region and the tissues (particularly cancerous ones) contain a large amount of interstitial water [6]. An infrared (IR) laser is integrated into a reflection-mode THz time-domain spectroscopic (THz-TDS) system to induce surface plasmon polaritons on the nanoparticles, thereby increasing the temperature of water in the tissue containing the nanoparticle contrast. A highly sensitive THz reflection signal was observed in tissues incorporated with nanoparticles under the IR light. Moreover, a strong image contrast was obtained between tissues with and without nanoparticle contrast in the differential THz image [3].

However, THz-TDS systems were adopted in former THz molecular imaging techniques [2-5]. The system compositions for generation and coherent detection of THz pulses are rather complex for practical applications, especially for real-time monitoring of surgical processes in the operating room. Furthermore, a pixel-by-pixel imaging strategy is required to detect THz pulses and achieve sufficient IR laser intensity for exciting surface plasmon polaritons on the nanoparticles. The imaging speed with this approach is too low for practical applications. In addition, the THz pulses can be strongly absorbed by water vapor in the air for the high power absorption of water in the adopted THz region (0.1-3 THz) [6].

In this study, we propose a low-cost, simple, and stable SPIOs enhanced continuous-THz-wave imaging method. An alternative magnetic field generation equipment is integrated into a 0.2-THz reflective continuous-THz-wave imaging system, which enables real-time focal-plane imaging. The temperature of water around the SPIOs increases under the application of the alternative magnetic field. The refractive index and power absorption of water change significantly at 0.2 THz [6], which enhances the measurement sensitivity dramatically. Furthermore, the power absorption of water at 0.2 THz is relatively small [6], which is beneficial for practical application. To test the feasibility of this imaging method, the SPIO water solutions were used to simulate the THz response from cells after endocytosis of SPIOs.

Higher water temperature was achieved with higher SPIO solution density and alternative magnetic field strength, which generated a stronger reflected THz signal from the SPIO solution. The focal-plane THz imaging results demonstrated that the THz reflection images from water with and without SPIOs were nearly identical. Nevertheless, the image of water with SPIOs increased in brightness upon alternative magnetic field application when compared with the THz-only image, whereas there was almost no change in water without SPIOs. Furthermore, a surprising result emerged as regards the difference between the images before and after exposure to the alternative magnetic field.

The differential image of water without SPIOs was almost indecipherable, while a clear contrast was observed in the image of water with SPIOs.

From these results, we can conclude that the SPIO water solution can be differentiated (as indicated by the very high contrast) from the solution without SPIOs upon application of the alternative magnetic field. These preliminary results suggest that highly sensitive THz imaging for cancer diagnosis can be achieved with SPIO contrast agents. In addition, the demarcation of cancerous tumors can be identified as the differential signal and relative reflection changes emerging when phase-conjugated SPIOs are specifically targeted at the tumor. The in vivo THz imaging study of cancer with phase-conjugated SPIOs based on the proposed technique will be conducted in the near future. The method offers the advantages of low cost and simplicity of operation, and it is particularly suitable for real-time imaging applications. We believe that our proposed contrast-enhanced continuous-THz imaging modality can facilitate cancer diagnosis and monitoring of nanoparticle drug delivery.

References:

- [1] X. Yang, X. Zhao, K. Yang, Y. Liu, Y. Liu, W. Fu, and Y. Luo, "Biomedical applications of terahertz spectroscopy and imaging," *Trends Biotechnol.* 34(10), 810-824 (2016).
- [2] S. J. Oh, J. Kang, I. Maeng, J. Suh, Y. Huh, S. Haam, and J.-H. Son, "Nanoparticle-enabled terahertz imaging for cancer diagnosis," *Opt. Express* 17(5), 3469–3475 (2009).
- [3] S. J. Oh, J. Choi, I. Maeng, J. Y. Park, K. Lee, Y. Huh, J. Suh, S. Haam, and J.-H. Son, "Molecular imaging with terahertz waves," *Opt. Express* 19(5), 4009–4016 (2011).
- [4] J. Y. Park, H. J. Choi, G.-E. Nam, K.-S. Cho, and J.-H. Son, "In vivo dual-modality terahertz/magnetic resonance imaging using superparamagnetic iron oxide nanoparticles as a dual contrast agent," *IEEE Trans. Terahertz Sci. Technol.* 1(1), 93–98 (2012).
- [5] S. J. Oh, Y.-M. Huh, J.-S. Suh, J. Choi, S. Haam, and J.-H. Son, "Cancer diagnosis by terahertz molecular imaging technique," *J. Infrared Millim. Terahertz Waves* 33(1), 74–81 (2012).
- [6] C. Ronne, L. Thrane, P.-O. Åstrand, A. Wallqvist, K. V. Mikkelsen, and S. R. Keiding, "Investigation of temperature dependence of dielectric relaxation in liquid water by THz reflection spectroscopy and molecular dynamics simulation," *J. Chem. Phys.* 107(14), 5319–5331 (1997).

Study on bionic compound eyes imaging system in field stitching method

Zhao Yu¹, Liu Zhi-ying¹, Fu Yue-gang¹, Zhang Kai¹

¹ School of Opto-electronic Engineering, Changchun University of Science and Technology, Changchun 130022, China

Utilizing the multi-axis feature in compound eyes, a bionic compound eyes imaging system with a large field of view (FOV) has been investigated in this paper. Comparing with traditional compound eyes, this system used to target detection and recognition overcomes the defects of short sighting distance and small aperture. According to the sub-eye's focal length, its detector size and the required FOV of compound eye imaging system, the distribution periodic and arrangement positions of sub-eye systems have been determined so that compound eye imaging system has no blind area. The imaging system designed in this method is consisted of 31 subsystems with different resolutions, the largest FOV reach at 53.9° , the maximum and minimum angular resolution are 0.006° and 0.017° respectively. As shown in the imaging results of the experimental prototype with 13 sub-eye systems, the blind area is non-existent, the situation of field overlapping is consistent with simulation result by LightTools. It is verified that the design of bionic compound eye imaging system with 31 components is available. The field stitching method can be as a theoretical guide for bionic compound eye system design.

Keywords:

Bionic compound eye; Field stitching; Image system

Laser Doppler flowmetry and spectroscopy methods in assessment of microvascular and metabolic complications in diabetes

Elena V. Zharkikh¹, Victor V. Dremin¹, Evgeny A. Zharebtsov^{1,2}, Elena V. Potapova¹, Andrey V. Dunaev¹

¹ Orel State University named after I.S. Turgenev,

² Aston Institute of Photonic Technologies, Aston University

According to the International Diabetes Federation (IDF), the problem of early diagnosis of diabetes mellitus (DM) and its complications is one of the most acute in modern healthcare. Decreased perfusion, oxygen delivery and consumption are among the most important factors. The skin is easily amenable to research using various optical diagnostic methods that give an idea of the physiology and various pathologies of tissues. In this study a joint application of the laser Doppler flowmetry (LDF), fluorescence spectroscopy and diffuse reflectance spectroscopy methods was suggested. The aim of this work was to investigate the possibilities of optical non-invasive diagnostic methods in determining of microcirculatory and oxygen metabolism disorders in patients with DM.

Experimental studies of healthy volunteers and patients with DM were conducted. Two study protocols were used. The first part of the study involved 4 stages: registration of a basic test of LDF-record for a 4 min period, registration of a local cold test ($t=25\text{ }^{\circ}\text{C}$) and a local heating test ($t=35\text{ }^{\circ}\text{C}$) for a 4 min each, registration of a local heating test ($t=42\text{ }^{\circ}\text{C}$) for a 10 min. During each stage a pair of fluorescence spectra were registered (excitation wavelengths are 365 and 450 nm). The optical probe was installed on the dorsal surface of the foot on a point located on a plateau between the 1st and 2nd metatarsals. Before the beginning of each study at the specified point registration of the spectra of skin diffuse reflection was carried out by a compact spectrometer "FLAME" (Ocean Optics, USA). In addition, for patients with visible trophic disorders such as ulcers, spectra were recorded directly at ulcers and at one centimetre from ulcers (at the intact region). The next part of the study included another sequence of temperature effects. The study was conducted in three stages. Namely, they are follow: registration of the LDF-record and fluorescence signal in basal condition for 8 min, local cooling to $10\text{ }^{\circ}\text{C}$ for 1 min and then local heating to $35\text{ }^{\circ}\text{C}$ for 4 min. Parameter registration was not performed until the achievement of specified temperature. The optical probe was installed into the hole of Peltier element intended for thermal tests. Studies were carried out on the feet in places with glabrous and nonglabrous skin.

The result of the study revealed that the rate of the perfusion upon heating to 35 and 42 degrees for patients are statistically smaller ($Im_3 = 6.74 \pm 2.70\text{ PU}$; $Im_4 = 11.89 \pm 3.71\text{ PU}$) compared to control group ($Im_3 = 9.44 \pm 3.28\text{ PU}$; $Im_4 = 20.12 \pm 4.35\text{ PU}$), that may indicate insufficient re-regulation of blood-microcirculation system by mechanisms that provide vasodilation. Increased fluorescence intensity in patients in comparison to control group ($3.1 \pm 0.9\text{ a.u.}$ vs $2.2 \pm 0.8\text{ a.u.}$ and $2.3 \pm 1.1\text{ a.u.}$ vs $1.2 \pm 0.4\text{ a.u.}$ upon excitation using UV and blue light, respectively). This increase in fluorescence can be due to the accumulation of advanced glycation end products that may initiate expression of collagen genes and other proteins of the capillary membrane and skin. During the research it was also discovered that the highest blood circulation was observed in patients with focal disorders (66.9 a.u.). Erythema index for patients without ulcers was higher than that of volunteers from the control group (28.7 a.u. vs 13.3 a.u.), which may indicate the presence of disorders in the peripheral circulation.

The proposed approach showed high sensitivity in the detection of peripheral blood flow and oxidative metabolism disorders. The applied methods can be used as additional non-invasive diagnostic methods in endocrinology departments for long-term monitoring of patients' condition.

Octagonal-core and nodeless anti-resonant hollow-core fibers transmission spectra comparison

V.V. Demidov¹, S.O. Leonov², V.A. Ananyev^{1,3}, V.O. Tigaev², E.A. Yelistratova²

¹Research and Technological Institute of Optical Materials All-Russian Scientific Center "S.I. Vavilov State Optical Institute", 36/1 Babushkin str., St. Petersburg, 192171 Russia

²Science and Education Center for Photonics and IR-Technology at the Bauman Moscow State Technical University, 2-nd Baumanskaya str., Moscow, 105005 Russia

³Department of Optical Information Technologies and Materials at the ITMO University, 49 Kronverksky pr., St. Petersburg, 197101 Russia

E-mail: leonov-st@ya.ru

Abstract. We compare guiding properties of the two prominent silica-based anti-resonant hollow-core fiber concepts (negative curvature of the core/cladding boundary and nodeless capillary structure) for operating in the wavelength range 600 – 2400 nm. The transmission spectra and fundamental mode profiles were calculated and measured for both mentioned fiber designs.

1. Introduction

Hollow core fibers (HCFs) based on the anti-resonant guiding mechanism have been attracting much attention to their unique optical properties and potential interdisciplinary applications including highly efficient laser-matter interaction [1], ultra-short pulse delivery [2], pulse compression [3] and low-loss mid-infrared transmission [4]. There are several types of HCFs having either a typical photonic crystal cladding, Kagome lattice or a single cycle of capillaries around the core. In latter case it was shown that anti-resonant properties depend strongly on the core size and the shape of the core-cladding boundary [5].

In this paper, we demonstrate capabilities of the two prominent silica-based HCF concepts (negative curvature of the core boundary [6] and nodeless tube lattice structure [7]) to perform low-loss transmission both in the near- and mid-infrared spectral regions.

2. Fiber properties

Two different types of HCFs were fabricated using the conventional stack-and-draw technique.

The first fiber was designed from eight touching capillaries providing the octagonal shape of the core (Sample 1) and was characterized by the core diameter of 52 μm , outer diameter of 200 μm and a wall thickness at the core boundary $\sim 1.5 \mu\text{m}$. The negative curvature of the core/cladding boundary was obtained by putting an excess gas pressure inside capillaries during the drawing process. Using the FEM simulation, it was determined that the fiber localizes the fundamental mode mostly in the core area. The second fiber had the nodeless capillary structure (Sample 2) with the core diameter of 46 μm , outer diameter of 130 μm and a wall thickness at the core boundary $\sim 2.0 \mu\text{m}$. The fiber was produced from six non-touching capillaries placed inside the base tube. As in the first case, the gas pressure was controlled carefully in order to keep all capillaries separately from each other.

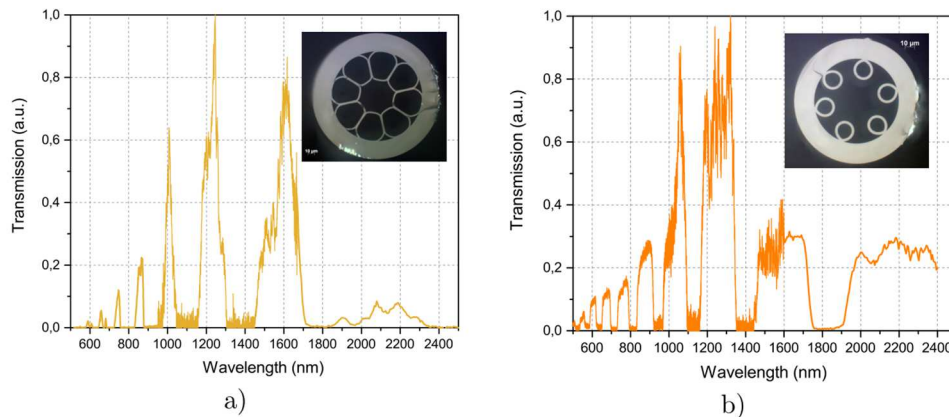


Figure 1. Measured transmission spectra of the octagonal-core negative curvature (a) and nodeless capillary structure (b) HCFs. Inset: microscope image of the fabricated fibers.

Measured transmission spectra of the octagonal-core negative curvature (a) and nodeless capillary structure (b) HCFs. Inset: microscope image of the fabricated fibers. The transmission spectra of the fibers (Fig. 1) were measured by passing light from the tungsten halogen lamp through the samples of 35 cm long. The output signal were registered by three optical spectrometers operating in wavelength regions of 600 – 1000 nm (Thorlabs CCS200), 900 – 1700 nm (YOKOGAWA AQ6370C), 1000 – 2500 nm (Avantes AvaSpec-NIR256-TEC).

As can be seen on Fig. 1, Sample A has transmission windows at wavelength of 1000/1250/1600/2150 nm and Sample B – at 1050/1300/1600/2200 nm. The mid-infrared window for Sample B is larger and more pronounced in terms of relative transmission due to the larger thickness of silica walls at the core/cladding boundary. In addition, the Sample B is predicted to be practically single-mode at the wavelength 2.45 μm (applicable with the Cr²⁺:ZnSe laser source [8]) as the losses of the most competitive higher-order modes (LP₁₁, LP₂₁, LP₀₂ and LP₃₁) tend to be above 1 dB/m.

3. Conclusions

In summary, two types of silica-based anti-resonant hollow-core fibers (negative curvature of the core/cladding boundary and nodeless capillary structure) with the core size $\sim 50 \mu\text{m}$ were designed and implemented. The transmission spectra of the fibers within the wavelength range 600 – 2400 nm were measured. The fiber with the nodeless capillary structure performed better mid-infrared transmission due to the thicker silica wall at the core/cladding boundary.

References:

- [1] Russell P S J, Holzer P, Chang W, Abdolvand A and Travers J C 2014 *Nature Photonics* **8** 278–286
- [2] Jaworski P, Yu F, Carter R M, Knight J C, Shephard J D and Hand D P 2015 *Opt. Express* **23** 8498–8506
- [3] Mak K F, Seidel M, Pronin O, Frosz M H, Abdolvand A, Pervak V, Apolonski A, Krausz F, Travers J C and Russell P S J 2015 *Opt. Lett.* **40** 1238–1241
- [4] Yu F, Wadsworth W J and Knight J C 2012 *Opt. Express* **20** 11153–11158
- [5] Pryamikov A D, Alagashev G K, Kosolapov A F and Biriukov A S 2016 *Laser Physics* **26** 125104
- [6] Pryamikov A D, Biriukov A S, Kosolapov A F, Plotnichenko V G, Semjonov S L and Dianov E M 2011 *Opt. Express* **19** 1441–1448
- [7] Poletti F 2014 *Opt. Express* **22** 23807–23828
- [8] Sorokina I T and Sorokin E 2015 *IEEE Journal of Selected Topics in Quantum Electronics* **21** 273–291

Application and possibilities of fluorescence spectroscopy method for intraoperative analysis of abdominal cavity organs tissues during minimally invasive interventions

Ksenia Kandurova¹, Victor Dremin¹, Evgeny. A. Zhrebtsov², Alexandr Alyanov^{1,3}, Andrian Mamoshin^{1,3}, Andrey Dunaev¹

¹ *Biomedical Photonics Laboratory of University Clinic, Orel State University named after I.S. Turgenev, Orel, Russia*

² *Aston Institute of Photonic Technologies, Aston University, Birmingham, UK*

³ *Department of X-ray-surgical methods of diagnosis and treatment, Orel Regional Clinical Hospital, Orel, Russia*

Currently, the number of patients with malignant tumors of hepatopancreatoduodenal area is growing. These pathologies have high level of complications and mortality and are hard to be detected at early stages. This is one of the most important problems of surgery of the abdominal cavity due to the high level of complications and mortality. Currently, the minimally invasive interventions are becoming more widespread as a main method of treatment of various pathologies of the abdominal organs. In this regard, there is a necessity to develop and implement new diagnostic methods and criteria for more detailed monitoring of the tissues state during treatment.

Optical non-invasive diagnostic methods are becoming widespread in clinical practice. One of them is fluorescence spectroscopy (FS). This method is based on analyzing the autofluorescence specters of endogenous fluoroforesin biological tissues induced with optical radiation [1,2]. It is known that one of consequences of cells functioning violation are changes in a respiratory chain of mitochondria, which result in changes in accumulation of NADH and FAD coenzymes. Oncological processes can also be accompanied by structural changes in collagen fibers in the hollow organs stroma. Potentially, all these changes can be assessed in vivo by means of the FS method [3].

Thus, the aim of this work is to study the possibility of applying fluorescence spectroscopy to assess metabolic activity of the abdominal cavity organs tissues in diseases of hepatopancreatoduodenal area.

Experimental measurements were conducted using the fluorescence channel of specially designed fiber-optic system with a laparoscopic optical probe (SPE "LAZMA" Ltd, Russia). A 365 nm and 450 nm radiation sources were used for fluorescence excitation. A total of 25 patients of Orel Regional Clinical Hospital department of X-ray-surgical methods of diagnosis and treatment aged 66 ± 10 years were engaged in the research. Areas of interest were distal and proximal parts on common bile duct, neck, body and fundus of gallbladder, wall and cavity of hepatic abscess and pancreas. Fluorescence spectra were recorded during primary and repeated minimally invasive interventions.

As a result, fluorescence spectra for each excitation wavelength and each area were obtained and normalized to the backscattered source signal. Processing of the data has shown that intensity of fluorescence and backscattered radiation can greatly vary in different areas of interest. It was observed in different points of one area as well. A number of factors causes it: the state and kind of tissue changes, the phase development of pathological processes, the stage of treatment, the presence of blood, pus and other substances. The differences with respect to the healthy tissues were associated with the presence of tumour or inflammation.

Thus, the results of the work show that fluorescence spectroscopy can be used for assessing the state of tissues during minimally invasive interventions in vivo. Obtained data show high sensitivity of this method to a number of factors. That way, there is a necessity to conduct further research to determine the influence of each factor on obtained spectra. It will allow to interpret the results more properly and to develop new diagnostic criteria for the study and treatment of hepatopancreatoduodenal organs pathologies.

References:

- [1] Lakowicz, J. R., "Principles of Fluorescence Spectroscopy", (Kluwer Academic Publishers, New York, 2006).
- [2] M. A. Mycek, B. W. Pogue, "Handbook of Biomedical Fluorescence", (CRC Press, 2003).
- [3] V. V. Tuchin, "Tissue optics: Light scattering methods and instruments for medical diagnosis:Third edition" (SPIE PRESS BOOK, 2015).

Blood glucose concentration sensing using THz spectroscopy

S. I. Gusev¹, P. S. Demchenko¹, and M. K. Khodzitsky¹

¹ ITMO University, Russia

Diabetes mellitus is a group of metabolic diseases characterized by hyperglycemia resulting from defects in insulin secretion, insulin action, or both [1]. There is a direct relationship between the level of glucose in the blood of patients with diabetes and the probability of developing complications of the disease [2]. Accurate and efficient assessment of blood glucose concentration is critical in clinical management of many pathological conditions in human population.

One of the most important benefits of terahertz spectroscopy methods is the possibility of non-invasive analysis of biological samples [3]. Transmission mode of spectroscopy is common way for collecting data about easy extractable media. On the one hand transmission mode of medium analysis provides accurate results, but can be unsuitable for completely non-invasive investigation of biological tissues and fluids [4,5]. On the other hand, reflection mode of spectroscopy cannot be used for direct blood optical measurement due to the location of blood below the surface of the human body. Moreover, THz reflected signal considerably weakened due to the water contained in the skin layer. Despite this, capillary blood located in fingers' nail beds may be investigated through the nails in the reflection mode.

In this paper we present the results of THz spectra measurements of nails and whole blood samples with different glucose concentration. Our THz spectrometer has been described previously [4,5]. We investigated the frequency dispersions of complex refractive index (η_{real} and η_{imag}), absorption coefficient (α), penetration depth (L) complex permittivity (ϵ_{real} and ϵ_{imag}) in the frequency range of 0.2 to 2.0THz. Analysis of the experimental spectra was performed by comparing spectra of biological samples with a Debye model of the dielectric function of water.

Observed results highlight the prospective of the described technique use for medical diagnosis of diabetes.

References:

- [1] "Classification and diagnosis of diabetes," *Diabetes Care*, Vol. 38, S8, 2014.
- [2] Ceriello, A. and S. Colagiuri, "International diabetes federation guideline for management of postmeal glucose: A review of recommendations," *Diabetic Medicine*, Vol. 25, No. 10, 115, 2008.
- [3] Pickwell, E., B. Cole, A. Fitzgerald, M. Pepper, and V. Wallace, "In vivo study of human skin using pulsed terahertz radiation," *Physics in Medicine and Biology*, Vol. 49, No. 9, 1595, 2004.
- [4] Gusev, S., M. Borovkova, M. Strepitov, and M. Khodzitsky, "Blood optical properties at various glucose level values in THz frequency range," *SPIE Proceedings*, Vol. 9537, 95372A, 2015.
- [5] Gusev, S., N. Balbekin, E. Sedykh, Y. A. Kononova, E. Litvinenko, A. Goryachuk, V. Begaeva, A. Y. Babenko, E. Grineva, and M. Khodzitsky, "Influence of creatinine and triglycerides concentrations on blood optical properties of diabetics in THz frequency range," *Journal of Physics: Conference Series*, Vol. 735, No. 1, 012088, 2016.